CRISPR-Cas9 Screening of Kaposi's Sarcoma-Associated Herpesvirus-Transformed Cells Identifies XPO1 as a Vulnerable Target of Cancer Cells

Marion Gruffaz,[a] Hongfeng Yuan,[a] Wen Meng,[b] Hui Liu,[a] Sangsu Bae,[c] Jin-Soo Kim,[d,e] Chun Lu,[f] Yufei Huang,[g] Shou-Jiang Gao[a,b,f,h]

[a]Department of Molecular Microbiology and Immunology, Keck School of Medicine, University of Southern California, Los Angeles, California, USA

[b]UPMC Hillman Cancer Center, Department of Microbiology and Molecular Genetics, University of Pittsburgh, Pittsburgh, Pennsylvania, USA

[c]Department of Chemistry, Hanyang University, Seoul, South Korea

[d]Center for Genome Engineering, Institute for Basic Science, Daejon, South Korea

[e]Department of Chemistry, Seoul National University, Seoul, South Korea

[f]Nanjing Medical University, Nanjing, China

[g]Department of Electrical and Computer Engineering, University of Texas at San Antonio, San Antonio, Texas, USA

[h]Laboratory of Human Virology and Oncology, Shantou University Medical College, Shantou, China

ABSTRACT The abnormal proliferation of cancer cells is driven by deregulated oncogenes or tumor suppressors, among which the cancer-vulnerable genes are attractive therapeutic targets. Targeting mislocalization of oncogenes and tumor suppressors resulting from aberrant nuclear export is effective for inhibiting growth transformation of cancer cells. We performed a clustered regularly interspaced short palindromic repeat (CRISPR)-associated (Cas) screening in a unique model of matched primary and oncogenic Kaposi's sarcoma-associated herpesvirus (KSHV)-transformed cells and identified genes that were growth promoting and growth suppressive for both types of cells, among which exportin XPO1 was demonstrated to be critical for the survival of transformed cells. Using XPO1 inhibitor KPT-8602 and by small interfering RNA (siRNA) knockdown, we confirmed the essential role of XPO1 in cell proliferation and growth transformation of KSHV-transformed cells and in cell lines of other cancers, including gastric cancer and liver cancer. XPO1 inhibition induced cell cycle arrest through p53 activation, but the mechanisms of p53 activation differed among the different types of cancer cells. p53 activation depended on the formation of promyelocytic leukemia (PML) nuclear bodies in gastric cancer and liver cancer cells. Mechanistically, XPO1 inhibition induced relocalization of autophagy adaptor protein p62 (SQSTM1), recruiting p53 for activation in PML nuclear bodies. Taken the data together, we have identified novel growth-promoting and growth-suppressive genes of primary and cancer cells and have demonstrated that XPO1 is a vulnerable target of cancer cells. XPO1 inhibition induces cell arrest through a novel PML- and p62-dependent mechanism of p53 activation in some types of cancer cells.

IMPORTANCE Using a model of oncogenic virus KSHV-driven cellular transformation of primary cells, we have performed a genome-wide CRISPR-Cas9 screening to identify vulnerable genes of cancer cells. This screening is unique in that this virus-induced oncogenesis model does not depend on any cellular genetic alterations and has matched primary and KSHV-transformed cells, which are not available for similar screenings in other types of cancer. We have identified genes that are both growth promoting and growth suppressive in primary and transformed cells, some of which could represent novel proto-oncogenes and tumor suppressors. In particular, we have demonstrated that the exportin XPO1 is a critical factor for the survival of

transformed cells. Using a XPO1 inhibitor (KPT-8602) and siRNA-mediated knock-down, we have confirmed the essential role of XPO1 in cell proliferation and in growth transformation of KSHV-transformed cells, as well as of gastric and liver cancer cells. XPO1 inhibition induces cell cycle arrest by activating p53, but the mechanisms of p53 activation differed among different types of cancer cells. p53 activation is dependent on the formation of PML nuclear bodies in gastric and liver cancer cells. Mechanistically, XPO1 inhibition induces relocalization of autophagy adaptor protein p62 (SQSTM1), recruiting p53 for activation in PML nuclear bodies. These results illustrate that XPO1 is a vulnerable target of cancer cells and reveal a novel mechanism for blocking cancer cell proliferation by XPO1 inhibition as well as a novel PML- and p62-mediated mechanism of p53 activation in some types of cancer cells.

KEYWORDS CRISPR-Cas9 screening, gastric cancer, human herpesvirus 8, HHV8, Kaposi's sarcoma, Kaposi's sarcoma-associated herpesvirus, KSHV, liver cancer, PML bodies, SQSTM1, p62, XPO1, p53

The malfunction of nuclear transport, which shuttles proteins between cytoplasm and nucleus, often leads to mislocalization of oncogenes and tumor suppressor proteins in cancer cells (1). Indeed, numerous proteins involved in cancer, including p53, adenomatous polyposis coli (APC), retinoblastoma (Rb), NFAT (nuclear factor of activated T cells), and β-catenin, are abnormally localized in cancer cells. The consequence of these dysfunctions is either overactivation of oncogenes or inactivation of tumor suppressor proteins, resulting in uncontrolled cell proliferation and growth transformation (2).

Unlike passive diffusion of metabolites, shuttling of proteins between nucleus and cytoplasm is an active, highly regulated receptor-mediated process. The nuclear pore complex (NPC) is a supramolecular structure composed of more than 30 nucleoporins interacting with importins and exportins within the NPC channel. The directionality of the transport depends on the distribution of GTP- or GDP-bound GTPase, the Ran protein, in both cytoplasmic and nucleic compartments (3). Indeed, while importins bind to their cargo proteins in cytoplasm and release them in nucleus upon binding of RanGTP, exportins bind to cargos in nucleus only in the presence of RanGTP and release them in cytoplasm upon Ran-driven GTP hydrolysis (4).

The exportin family consists of 7 members, including XPO1 (CRM1), XPO2 (CSE1L), XPO3 (XPOt), XPO4, XPO5, XPO6, and XPO7. While XPO1, XPO2, XPO4, XPO6, and XPO7 primarily mediate the export of cargo proteins, XPO3 and XPO5 are involved in the transport of tRNAs and precursor microRNAs (pre-miRNAs), respectively. XPO1, the major protein export receptor, is also associated with the nuclear export of mRNAs and rRNAs (5).

Mechanistically, XPO1 interacts with the nucleoporins NUP214 and NUP88 inside the NPC and exports proteins containing XPO1-specific nuclear export signal (NES) sequences, which are short leucine-rich sequences. Several tumor suppressor proteins and oncogenes display XPO1-specific NES (6). Consequently, XPO1 dysregulation indirectly regulates cellular functions such as cell proliferation and cellular transformation, apoptosis, and chromosome segregation (2). In particular, XPO1 is upregulated in ovarian carcinoma, glioma, osteosarcoma, and pancreatic, cervical, and gastric cancers, resulting in induction of abnormal accumulation of the tumor suppressor proteins Rb, APC, p53, p21, and p27 in the cytoplasm, leading to losses of their nuclear functions (2). On the other hand, inhibition of XPO1 by RNA interference or with inhibitors, such as leptomycin B or selective inhibitors of nuclear export (SINE), prevents cellular transformation and tumorigenesis in numerous cancer models. Hence, XPO1 has become a promising target in cancer therapy (7).

Nuclear bodies (NBs) are membraneless structures within the nucleus involved in multiple pathways of genome maintenance. Among them, promyelocytic leukemia protein nuclear bodies (PML-NBs) are involved in DNA repair, DNA damage response,

telomere homeostasis, and p53-associated apoptosis and cell cycle arrest (8). Among the various biological consequences of XPO1 inhibition, several groups observed the retention of p53, the most extensively described tumor suppressor, in the nucleus, enhancing p53-mediated tumor suppressor activity (8). Indeed, activation of p53 induces cell cycle arrest and apoptosis in many types of cancer cells. In particular, inside the nucleus, p53 colocalizes and interacts with PML-NBs, which serve as p53 coactivators (9). PML knockout impairs p53-dependent apoptosis and p53-mediated transcriptional activation, as well as induction of p53 target genes such as Bax and p21 (9). Therefore, PML-NBs may play a significant role in apoptosis and cancer. Nevertheless, the underlying molecular mechanism mediating PML-dependent p53 activation is still unclear.

The development of new genome engineering technologies has enabled the identification of oncogenes and tumor suppressors in cancer cells *in vitro* and *in vivo* (10, 11). In particular, the clustered regularly interspaced short palindromic repeat (CRISPR)-associated (Cas) protein system, adapted to mammalian cells on the basis of a mechanism of adaptive immunity of bacteria and archaea, enhances the accessibility of genome manipulation by allowing the targeting of genes with specific RNA sequences (12). Briefly, CRISPR relies on Cas9 guided by single guide RNAs (sgRNAs; CRISPR RNAs) to induce loss-of-function (LOF) mutations via frameshifts in the coding region, leading to gene inactivation. The CRISPR-Cas9 system has enabled different types of genetic modifications, such as gene disruption and transcriptional activation. Several types of biological screens based on the CRISPR-Cas9 system have already been carried out to identify viral restriction factors, oncogenes, and tumor suppressors, as well as to develop T-cell immunotherapies.

In this study, by performing a genome-wide CRISPR-Cas9 screening of cells transformed by an oncogenic virus, namely, Kaposi's sarcoma-associated herpesvirus (KSHV), we have identified cellular genes that are essential for cellular transformation (13). Briefly, CRISPR pooled libraries containing sgRNAs that specifically target all known cellular genes were transduced into Cas9-expressing KSHV-transformed primary rat mesenchymal embryonic stem (KMM) cells and control primary rat mesenchymal stem (MM) cells (13). Genomic DNAs from surviving MM cells and KMM cells were collected at days 1, 4, 11, and 21 postransduction and sequenced, and the results were analyzed for the gain or loss of sgRNAs. We identified exportin family members XPO1, XPO2, XPO3, XPO5, and XPO7 as the essential factors involved in the survival of KMM cells. We confirmed the essential role of XPO1 in cell proliferation and growth transformation using cell lines of other types of cancer, including AGS cells derived from gastric cancer and HUH7 cells derived from liver cancer. We showed that inhibition of XPO1 by small interfering RNAs (siRNAs) or with a XPO1 inhibitor, KPT-8602, blocked cell proliferation and growth transformation by inducing p53-mediated cell cycle arrest in all types of cancer cells tested. However, we found that the mechanisms mediating p53 activation differed among different types of cancer cells. In AGS and HUH7 cells, p53 activation was correlated with nuclear accumulation of autophagy adaptor protein p62 (SQSTM1), which was colocalized with p53 within the PML-NBs. Knockdown of p62 with siRNAs abrogated p53 activation induced by XPO1 inhibition. These results highlight an essential role of p62 in controlling cell proliferation and growth transformation by mediating activation of the p53 pathway in some types of cancer cells.

RESULTS

Genome-wide CRISPR-Cas9 screening for essential genes of KSHV-transformed cells. KSHV is an oncogenic virus which regulates numerous growth-promoting and survival pathways (14). We have previously shown that infection by KSHV alone is sufficient to efficiently infect and transform MM cells without depending on cellular genetic alterations and that KSHV-transformed KMM cells can efficiently induce tumors in nude mice with pathological features resembling Kaposi's sarcoma (KS) (13). Because of the unique features of KSHV-induced cellular transformation and the available
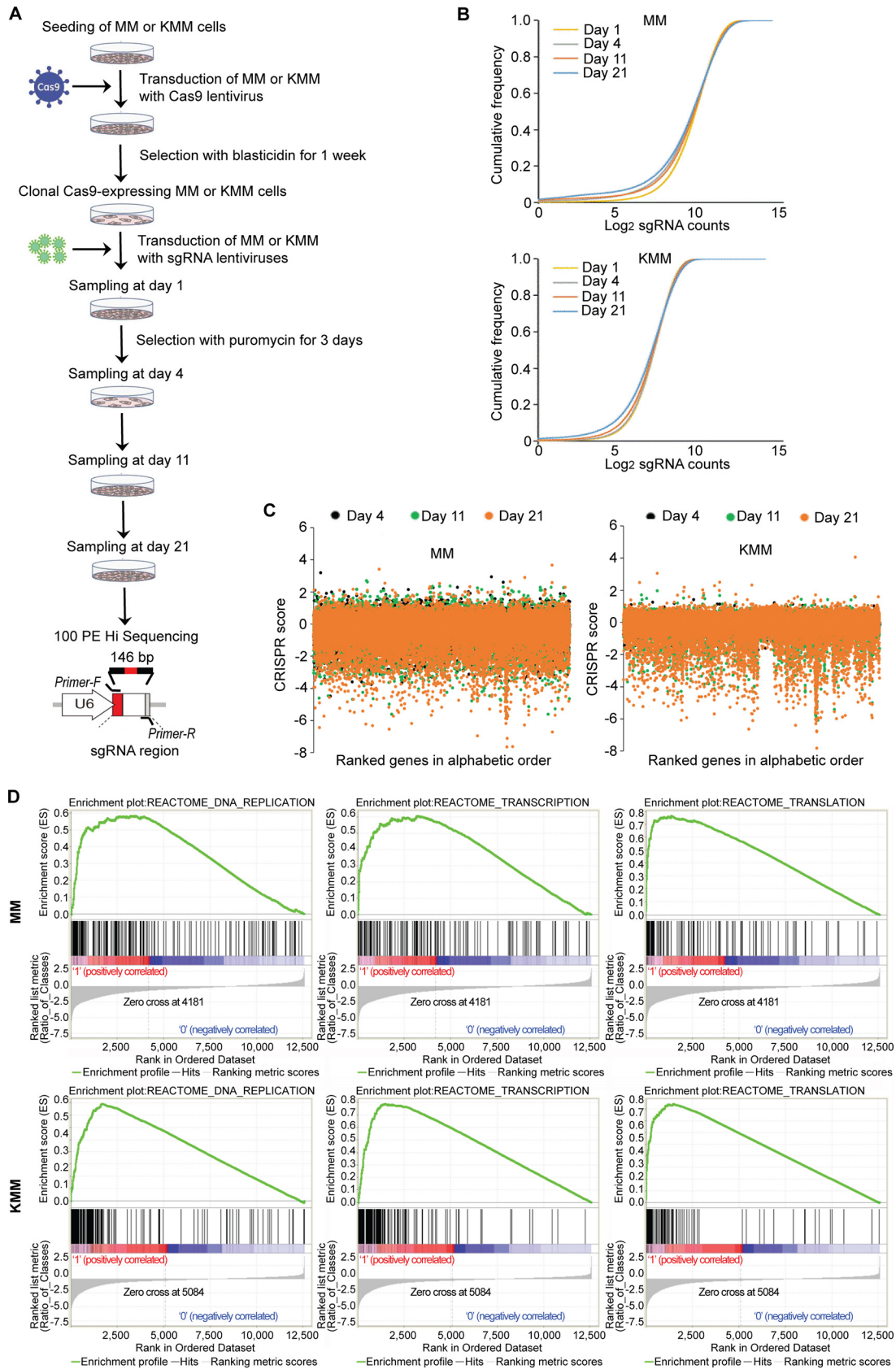
matched primary MM cells, KMM cells are ideal for identifying essential cellular genes that mediate growth transformation.

We first generated MM cells and KMM cells stably expressing Cas9 by lentiviral transduction following by positive selection with blasticidin for 1 week. Interestingly, we repeatedly observed weaker expression of Cas9 protein in MM cells than in KMM cells in multiple experiments (see Fig. S1A in the supplemental material). This was likely due to a higher rate of cell proliferation of KMM cells than of MM cells, often leading to higher expression levels of genes (13, 15). Despite the differential levels of Cas9 expression, we observed efficient inhibition of the endogenous SIRT1 expression after lentiviral transduction of sgRNAs targeting SIRT1 in both Cas9-expressing MM cells and KMM cells (Fig. S1B). Importantly, Cas9 expression did not affect the efficiency of colony formation of KMM cells in soft agar (Fig. S1C). As expected, Cas9-expressing MM cells did not form any colonies in soft agar (13). These results indicate that the Cas9-expressing MM cells and KMM cells can be used for identifying essential cellular genes that mediate growth transformation.

We then generated a library of sgRNAs targeting 19,840 genes of the rat genome, each with 3 independent sgRNAs. Cas9-expressing MM cells and KMM cells were transduced with the lentiviral sgRNA library and selected for 3 days with puromycin. The cultures were then switched to normal medium without any selection, and cell samples were collected at days 1, 4, 11, and 21 and subjected to DNA sequencing to determine the gain and loss sgRNAs over time (Fig. 1A). Cumulative frequencies of sgRNAs were analyzed at days 1, 4, 11, and 21 posttransduction in MM cells and KMM cells (Fig. 1B). Compared to day 1, we observed a progressive shift to the left in the curves at days 4, 11, and 21 postransduction, indicating depletion of a subset of sgRNAs. By assessing the global gene vulnerability levels at days 4, 11, and 21 postransduction, we observed a lower abundance of essential genes, displaying as negative CRISPR scores, in KMM cells than in MM cells, suggesting that KMM cells had higher survival rates than MM cells (Fig. 1B), which was also shown by the CRISPR scores of individual genes (Fig. 1C). Interestingly, the correlation between CRISPR score and gene expression at the RNA level (16) was observed neither in MM cells nor in KMM cells (Fig. S2). Finally, gene set enrichment analysis (GSEA) data from day 21 versus day 1 postransduction revealed enrichments of gene signatures in housekeeping pathways, including DNA replication, transcription, and translation, whose levels were significantly higher in KMM cells than in MM cells, confirming that the MM cells were more susceptible to gene disruption than the KMM cells (Fig. 1D).

Identification of essential genes and pathways of KSHV-transformed cells by CRISPR-Cas9 screening. Since essential genes are likely to encode key regulators of cellular processes involved in the survival of cancer cells, several studies previously investigated the overlapping of essential genes across different cancer cell lines by CRISPR-Cas9 screening (17). Therefore, we correlated results from MM cells and KMM cells with those of previous studies in chronic myeloid leukemia (CML) cell lines (KBM7 and K562) and Burkitt's lymphoma cell lines (Raji and Jiyoye). We found a high degree of overlap in gene essentiality between KSHV-transformed cells and other types of cancer cells ($R^2 = \geq 0.29$) (Fig. 2A). On the other hand, the correlation of essential genes between the primary MM cells and other types of cancer cells remained low ($R^2 = \leq 0.09$).

We next classified the 19,840 genes based on CRISPR scores. For each type of cells, we first selected genes with CRISPR scores that were statistically different between day 21 and day 1 and then those with CRISPR scores that were statistically different between KMM and MM cells and obtained 9 groups of genes (Fig. 2B; see also Table S1 in the supplemental material). Group 1 consisted of 11 genes that had a significant increase in CRISPR score for KMM cells but a significant decrease in CRISPR score for MM cells; group 2 consisted of 680 genes that had a significant increase in CRISPR score for KMM cells but no significant change in CRISPR score for MM cells; group 3 consisted of 51 genes that had significant increases in CRISPR score for both KMM and MM cells; group 4 consisted of 402 genes that had no significant change in CRISPR score for KMM

FIG 1 Genome-wide CRISPR-Cas9 screening for essential genes of KSHV-transformed cells. (A) Experimental design of CRISPR-Cas9 high-throughput screening in KSHV-transformed cells (KMM) in and matched primary MM cells. (B) Analysis of the cumulative

cells but had a significant decrease in CRISPR score for MM cells; group 5 consisted of 16,558 genes that had no significant change in CRISPR score for both KMM and MM cells; group 6 consisted of 552 genes that had no significant change in CRISPR score for KMM cells but had a significant increase in CRISPR score for MM cells; group 7 consisted of 314 genes that had significant decreases in CRISPR score for both KMM and MM cells; group 8 consisted of 1,259 genes that had a significant decrease in CRISPR score for KMM cells but had no significant change in CRISPR score for MM cells; and group 9 consisted of 13 genes that had a significant decrease in CRISPR score for KMM cells but had a significant increase in CRISPR score for MM cells.

Of these 9 groups, genes in group 8 were likely essential or pro-oncogenic for KMM cells but not for MM cells; among them, 18 genes, including Naa38, Rpl9_like, Rpl23a, Spcs3, Hspa14_like, Nfyb, Eif2b2, Mrpl55, Pold1, Nup43, Lin52, Csnk1a1, Aldoa, Rpl6, Ddx6, Wdr74, Rars, and Cnot1, had CRISPR score ratios of ≤5 (−32-fold) at day 21 compared to day 1 for KMM cells. Genes in group 2 were likely growth suppressive for KMM cells but not MM cells. On the other hand, genes in group 4 were likely essential or growth promoting for MM cells but not KMM cells whereas genes in group 6 were likely growth suppressive for MM cells but not KMM cells, suggesting that KSHV might target these two sets of genes to allow the transformed cells to overcome the essential or growth-suppressive functions of these genes, respectively.
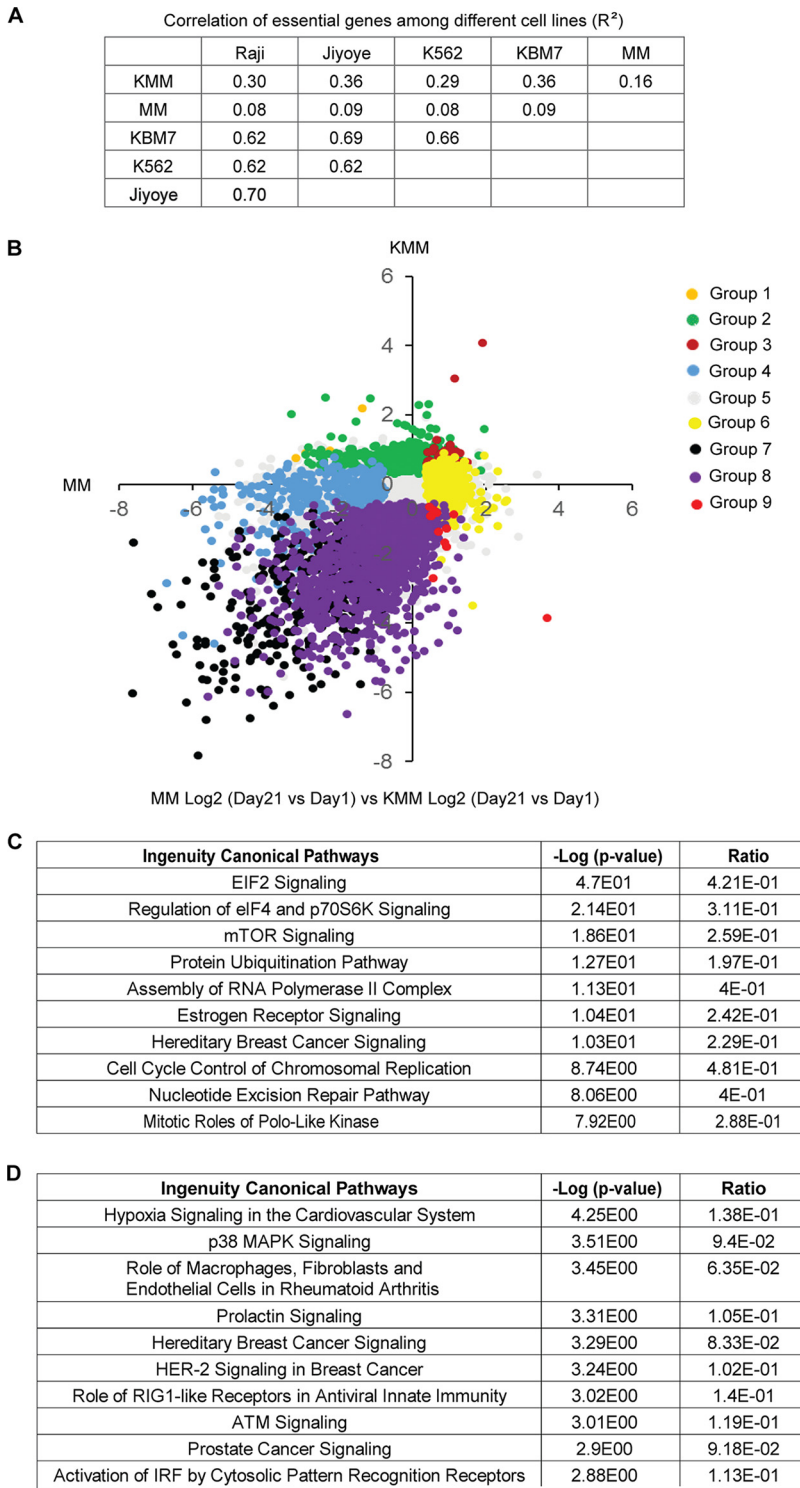
We determined the molecular pathways that were significantly depleted and enriched in KMM cells compared to MM cells (day 21 versus day 1) by Ingenuity pathway analysis (IPA) (see Table S2 and S3). We found that the eukaryotic initiation factor 2 (EIF2) pathway, the pathway controlling regulation of eIF4 and p70S6K, and the mTOR pathway were the top 3 depleted pathways in KMM cells compared to MM cells, highlighting their roles in the survival of the transformed cells (Fig. 2C). In fact, these pathways are highly related to one another, and the mTOR pathway is the most effective target for the treatment of KS (18), hence further validating the relevance of this model for KS. On the other hand, we found that the hypoxia pathway and the p38 mitogen-activated protein kinase (MAPK) pathway were the pathways that were most highly enriched in KMM cells compared to MM cells, suggesting their essential roles in maintaining the homeostasis of the KSHV-transformed cells (Fig. 2D).

Identification of XPO1 as a critical factor involved in cell proliferation and growth transformation of cell lines derived from multiple types of cancer. Since oncogenes and tumor suppressor proteins are often mislocalized as a result of dysregulation of nuclear transport (1), we focused on the exportin family members. The counts of sgRNAs of XPO1, XPO2, XPO3, and XPO5 significantly decreased at day 21 compared to day 1 in KMM cells, indicating the essential functions of these exportins, whereas XPO7 sgRNA counts significantly increased in KMM cells, indicating its putative antisurvival effect in the transformed cells (Fig. S3). In addition, MM cells were sensitive to XPO1, XPO2, and XPO5 knockout (Fig. S3). Numerous inhibitors have been developed for the main exportin member, XPO1. Some of these inhibitors are currently in clinical trials for different types of cancer (19–21). Hence, we decided to focus on this exportin.

Since XPO1 is upregulated in numerous types of cancer (22), we first examined XPO1 expression in KMM cells compared to MM cells. We observed 3-fold-higher expression level of XPO1 in KMM than in MM cells at the mRNA level (Fig. 3A), a finding that was confirmed at the protein level (Fig. 3B). Because KMM cells are latently infected by KSHV, expressing viral latent genes LANA, vFLIP, vCyclin, and the miRNA cluster (13, 23), we examined the roles of these genes in XPO1 expression. Deletion of either vCyclin or the miRNA cluster but not vFLIP abolished XPO1 upregulation (Fig. 3A and B). Because

FIG 1 Legend (Continued)
frequency of sgRNAs at days 1, 4, 11, and 21 postransduction in MM cells and KMM cells. (C) Analysis of gene essentiality at days 4, 11, and 21 postransduction using CRISPR scores in MM cells and KMM cells. Genes are ranked by alphabetical order. (D) GSEA of enriched pathways at day 21 versus day 1 postransduction in MM cells and KMM cells. PE Hi Sequencing, paired-end high-throughput sequencing.

A

Correlation of essential genes among different cell lines (R^2)

	Raji	Jiyoye	K562	KBM7	MM
KMM	0.30	0.36	0.29	0.36	0.16
MM	0.08	0.09	0.08	0.09	
KBM7	0.62	0.69	0.66		
K562	0.62	0.62			
Jiyoye	0.70				

B

MM Log2 (Day21 vs Day1) vs KMM Log2 (Day21 vs Day1)

C

Ingenuity Canonical Pathways	-Log (p-value)	Ratio
EIF2 Signaling	4.7E01	4.21E-01
Regulation of eIF4 and p70S6K Signaling	2.14E01	3.11E-01
mTOR Signaling	1.86E01	2.59E-01
Protein Ubiquitination Pathway	1.27E01	1.97E-01
Assembly of RNA Polymerase II Complex	1.13E01	4E-01
Estrogen Receptor Signaling	1.04E01	2.42E-01
Hereditary Breast Cancer Signaling	1.03E01	2.29E-01
Cell Cycle Control of Chromosomal Replication	8.74E00	4.81E-01
Nucleotide Excision Repair Pathway	8.06E00	4E-01
Mitotic Roles of Polo-Like Kinase	7.92E00	2.88E-01

D

Ingenuity Canonical Pathways	-Log (p-value)	Ratio
Hypoxia Signaling in the Cardiovascular System	4.25E00	1.38E-01
p38 MAPK Signaling	3.51E00	9.4E-02
Role of Macrophages, Fibroblasts and Endothelial Cells in Rheumatoid Arthritis	3.45E00	6.35E-02
Prolactin Signaling	3.31E00	1.05E-01
Hereditary Breast Cancer Signaling	3.29E00	8.33E-02
HER-2 Signaling in Breast Cancer	3.24E00	1.02E-01
Role of RIG1-like Receptors in Antiviral Innate Immunity	3.02E00	1.4E-01
ATM Signaling	3.01E00	1.19E-01
Prostate Cancer Signaling	2.9E00	9.18E-02
Activation of IRF by Cytosolic Pattern Recognition Receptors	2.88E00	1.13E-01

FIG 2 Identification of essential genes and pathways of KSHV-transformed cells. (A) Correlation of essential genes among MM, KMM, Raji, Jiyoye, K562, and KBM7 cell lines (R^2). (B) Classification of the 19,840 genes into 9 different groups based on the ratio of the CRISPR score at day 21 to the score at day 1 and statistical significance in results of comparisons MM versus KMM cells. Group 1 includes genes with KMM Log2 CRISPR scores of >0 and P values of <0.05 and with MM Log2 CRISPR scores of <0 and P values of <0.05; group 2 includes genes with KMM Log2 CRISPR scores of >0 and P values of <0.05 and MM Log2 CRISPR scores with P values of ≥0.05; group 3 includes genes with both MM and KMM Log2 CRISPR scores of >0 and P values of <0.05; group 4 includes genes with KMM Log2 CRISPR scores with P values of ≥0.05 and MM Log2 CRISPR scores of <0 and P values of <0.05; group 5 includes genes with both MM and KMM Log2 CRISPR scores with P values ≥0.05; group 6 includes genes with KMM Log2

(Continued on next page)

LANA is essential for KSHV episome persistence, we were not able to obtain cells latently infected by the LANA mutant (14). However, overexpression of LANA in MM cells did not alter XPO1 expression (results not shown). By complementing cells infected by the miRNA cluster deletion mutant (ΔmiR) with individual miRNAs, we found that pre-miR-K3 mediated XPO1 upregulation (Fig. 3C). Hence, both vCyclin, a homologue of cellular cyclin D2 (15), and pre-miR-K3, which activates the Akt pathway (24), not only promote cell cycle progression and facilitate the G_1/S-phase transition, respectively (15, 23), but also cause XPO1 upregulation.

We performed RNA interference knockdown to confirm the results obtained in CRISPR-Cas9 screening in KMM cells as well as in cell lines of other types of cancer, including AGS and HUH7 derived from gastric and liver cancers, respectively. The role of XPO1 in gastric cancer has not been examined before and has been examined in liver cancer only minimally (25). Knockdown of XPO1 decreased cell proliferation in KMM, AGS, and HUH7 cells but had no effect on the primary MM cells (Fig. 3D to F). Using XPO1-specific SINE compound KPT-8602, we observed significant inhibition of cell proliferation that occurred in a dose-dependent fashion starting at 0.1 μM in KMM cells and at 0.5 μM in AGS and HUH7 cells (Fig. 3G). MM cells were sensitive to KPT-8602 only at concentrations of >1 μM. Furthermore, inhibition of XPO1 abrogated colony formation of KMM, AGS, and HUH7 cells in soft agar (Fig. 3H), indicating the essential role of XPO1 in maintaining cellular transformation.

Inhibition of XPO1 induces p53 activation and cell cycle arrest. We examined the molecular mechanism mediating the inhibition of cell proliferation by KPT-8602. Treatment of MM, KMM, AGS, and HUH7 cells with KPT-8602 at 1 μM for 24 h induced cell cycle arrest at the G_2/M phase in MM and KMM and at the G_0/G_1 phase in AGS and HUH7 cells (Fig. 4A), suggesting different responses of these cells to KPT-8602. In parallel, we observed an activation of the p53 pathway as shown by the increase of phospho-p53 in KMM, AGS, and HUH7 cells but not MM cells after treatment with 1 μM KPT-8602 for 24 h (Fig. 4B). p53 activation has been shown to be dependent on PML-NBs within the nucleus. Interestingly, both MM cells and KMM cells had strong nuclear PML staining as well as cytoplasmic staining, with some cells showing staining patterns similar to those seen with PML-NB, and KPT-8602 treatment did not alter the PML staining pattern in those cells (Fig. 4C). These results indicated that PML-NBs were unlikely to mediate p53 activation in KMM cells. In contrast, AGS cells had no nuclear PML staining and only some HUH7 cells had weak nuclear PML staining, none of which showed the staining pattern of PML-NBs (Fig. 4C). However, a pattern of strong nuclear staining with PML-NBs was observed following KPT-8602 treatment in AGS and HUH7 cells (Fig. 4C). Significantly, siRNA knockdown of PML (Fig. 4D), which disrupted PML-NBs, inhibited KPT-8602-induced p53 phosphorylation in AGS and HUH7 cells, highlighting the essential role of PML-NBs in p53 activation in these cells (Fig. 4E).

p53 activation in PML-NBs depends on the nuclear accumulation of autophagy adaptor protein p62 (SQSTM1) in AGS and HUH7 cells. Since PML-NBs are thought to form hybrid bodies with p62 protein during cellular stress (26), we investigated the p62 protein after XPO1 inhibition in AGS and HUH7 cells. Treatment with 1 μM KPT-8602 for 24 h increased the expression level of p62 in AGS and HUH7 cells (Fig. 5A). Interestingly, we observed nuclear translocation and accumulation of p62, which was colocalized with p53 in AGS and HUH7 cells after KPT-8602 treatment (Fig. 5B). Furthermore, p62 was colocalized with PML-NBs in AGS and HUH7 cells following XPO1 inhibition, which was consistent with the hypothesis of formation of hybrid bodies

FIG 2 Legend (Continued)
CRISPR scores with P values of ≥0.05 and MM Log2 CRISPR scores of >0 and P values of <0.05; group 7 includes genes with both MM and KMM Log2 CRISPR scores of <0 and P values of <0.05; group 8 includes genes with KMM Log2 CRISPR scores of <0 and P values of <0.05 and MM Log2 CRISPR scores with P values of ≥0.05; group 9 includes genes with KMM Log2 CRISPR scores of <0 and P values of <0.05 and MM Log2 CRISPR scores of >0 and P values of <0.05. (C) IPA of top 10 depleted pathways in KMM cells over MM cells at day 21 versus day 1 posttransduction. (D) IPA of top 10 enriched pathways in KMM cells over MM cells at day 21 versus day 1 posttransduction.
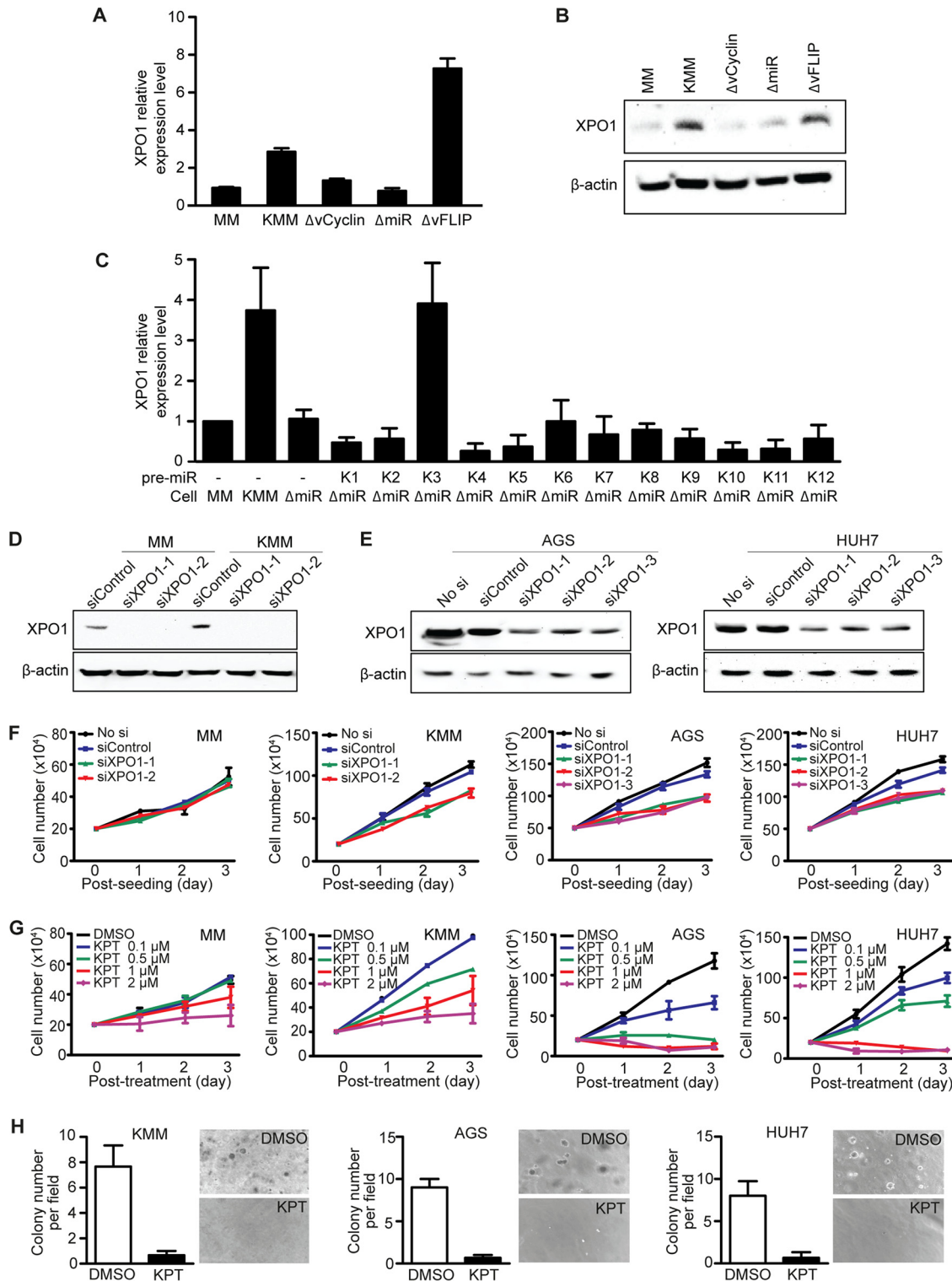
FIG 3 Identification of XPO1 as a vulnerable gene of KSHV-transformed KMM cells and of cell lines of gastric cancer AGS and liver cancer HUH7 cells. (A and B) XPO1 expression in MM cells and in MM cells infected by KSHV (KMM) and by mutant viruses with a deletion of vFLIP (ΔvFLIP), vCyclin (ΔvCyclin), or a cluster of 10 pre-miRNAs (ΔmiR) analyzed by reverse transcription-quantitative PCR (qRT-PCR) (A) and Western blotting (B). (C) Expression of XPO1 analyzed by qRT-PCR in MM cells, KMM cells, ΔmiR cells, or ΔmiR cells complemented with individual KSHV pre-miRNAs (K1 to K12). (D) Expression of XPO1 following siRNA knockdown analyzed by Western blotting in MM cells and KMM cells. (E) Expression of XPO1 following siRNA knockdown analyzed by Western blotting in AGS and HUH7 cells. (F) Analysis of cell proliferation following siRNA knockdown of XPO1 in MM, KMM, AGS, and HUH7 cell lines. (G) Analysis of cell proliferation following treatment with DMSO or KPT-8602 at different concentrations for 3 days in MM, KMM, AGS, and HUH7 cells. (H) Formation of colonies in soft agar following treatment with DMSO or KPT-8602 at 1 μM in KMM, AGS, and HUH7 cells. Representative fields are shown, and efficiencies of colony formation are presented.
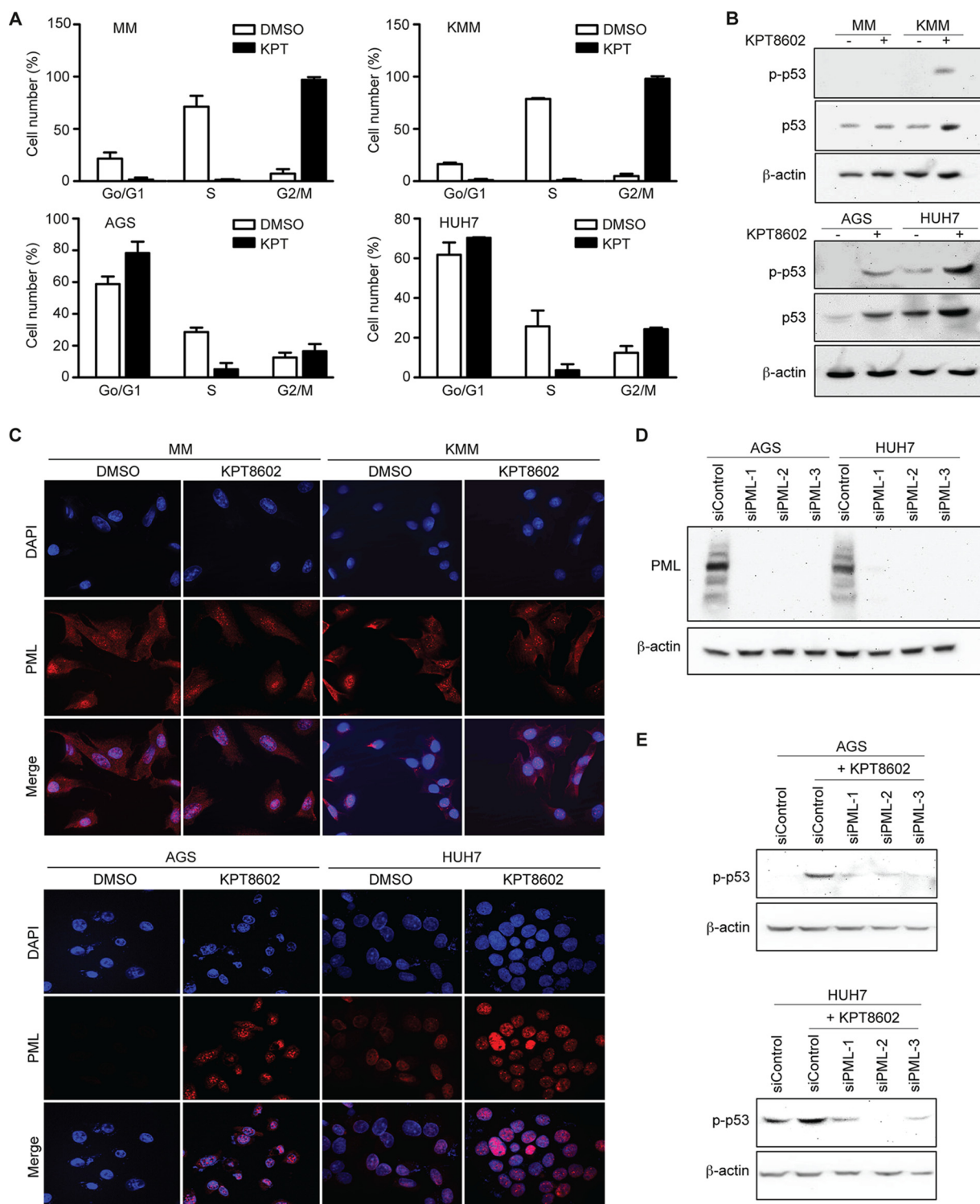
FIG 4 Inhibition of XPO1 induces PML-mediated p53 activation and cell cycle arrest. (A) Effect of KPT-8602 treatment on cell cycle progression of MM, KMM, AGS, and HUH7 cells. Cells treated with 1 μM KPT-8602 for 48 h were analyzed by flow cytometry after BrdU and propidium iodide staining. (B) Analysis of phospho-p53 (p-p53) and total p53 in MM, KMM, AGS, and HUH7 cells after treatment with 1 μM KPT-8602 by Western blotting. (C) Examination of PML in MM, KMM, AGS, and HUH7 cells after treatment with 1 μM KPT-8602 for 24 h by immunofluorescence assay. The slides were counterstained with DAPI, and pictures were taken with a confocal microscopy (magnification, ×600). (D) Expression of PML in AGS and HUH7 cells following siRNA knockdown analyzed by Western blotting. (E) Analysis of p-p53 in AGS and HUH7 cells following siRNA knockdown of PML analyzed by Western blotting.
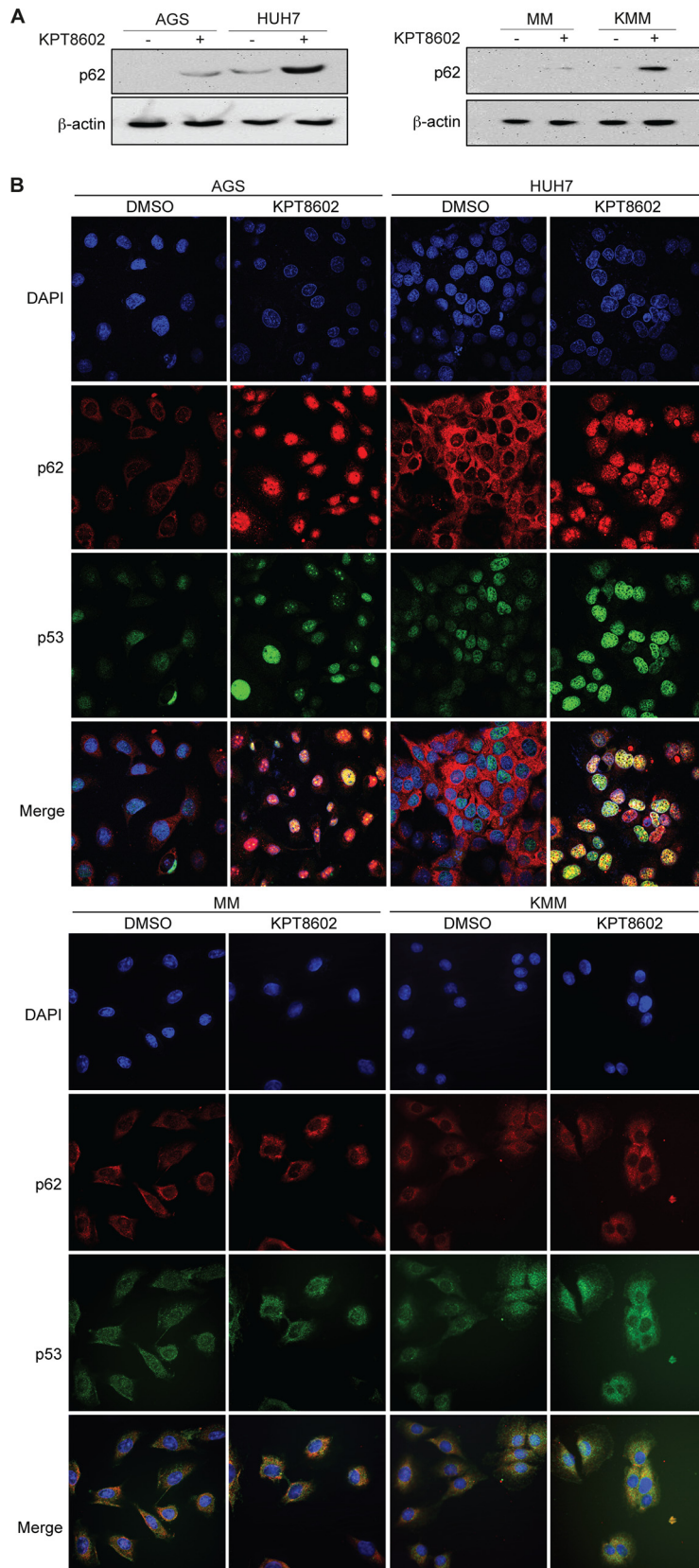
FIG 5 Induction of p62 nuclear accumulation and colocalization with p53 following XPO1 inhibition in AGS and HUH7 cells. (A) Expression of p62 in MM, KMM, AGS, and HUH7 cells after treatment with 1 μM KPT-8602 for 24 h analyzed by Western blotting. (B) Expression of p53 and p62 in AGS, HUH7, MM, and

(Continued on next page)

(Fig. 6A). The expression level of p62 was also increased in KMM cells but not in MM cells (Fig. 5A). However, we did not observe nuclear translocation and accumulation of p62 in MM cells and KMM cells, and there was no nuclear colocalization of p53 with p62 in these cells (Fig. 5B). Consistent with these results, there was no obvious nuclear colocalization of p62 with PML-NBs in MM cells and KMM cells (Fig. 6A). These results indicated that p62 was unlikely to be involved in p53 activation following XPO1 inhibition in KMM cells.

To investigate the role of p62 in p53 activation in AGS and HUH7 cells, we performed knockdown of p62 in AGS and HUH7 cells (Fig. 6B). Knockdown of p62 abolished p53 activation in AGS cells and significantly decreased p53 activation in HUH7 cells following treatment with KPT-8602 (Fig. 6C). These results indicate an essential role of p62 accumulation in XPO1 inhibition-induced p53 activation in PML-NBs in AGS and HUH7 cells.

DISCUSSION

Numerous genetic engineering techniques using endonucleases to induce double-stranded breaks (DSBs) at specific sites in the target DNA have been developed in the last few decades. Endonucleases, such as transcription activator-like effector nucleases (TALENs) or zinc finger nucleases (ZFNs), were previously used to inactivate targeted genes, but some studies highlighted their lack of specificity and poor efficiency (27). More recently, CRISPR-Cas9 has been shown to be an efficient and precise tool for genetic disruption or correction *in vitro* and *in vivo* (10, 11).

In this report, by performing a genome-wide CRISPR-Cas9 screening, we characterized gene essentiality in KSHV-transformed cells (13). KSHV, as a human oncogenic virus in the family of Herpesviridae, is associated with several human malignancies, including KS, primary effusion lymphoma (PEL), KSHV inflammatory cytokine syndrome (KICS), and a subset of multicentric Castleman's disease (MCD) (28). Using a model of KSHV-induced cellular transformation of primary cells (13), we have identified essential genes in both MM cells and KMM cells and observed an increase in survival ability in KSHV-transformed cells compared to primary cells in a genome-wide CRISPR-Cas9 knockout screening (Fig. 1), confirming the oncogenic nature of the virus. Moreover, we have identified genes involved in the survival of KMM or MM cells (Fig. 2). In parallel, we have observed a significant positive correlation in gene essentiality between KMM cells and other cancer cells observed by similar CRISPR-Cas9 screening (17), illustrating the convergence of common survival features in these cancer cells.

Current therapies targeting latent infections of oncogenic viruses are often limited in efficacy and cannot eradicate the viruses. Numerous studies have performed CRISPR-Cas9 screening in viral cancer models to identify novel therapeutic targets (29). CRISPR-Cas9 genome editing in models of oncogenic viruses should facilitate the identification of vulnerable genes/mutations, viral and cellular oncoproteins, and essential or restriction factors for infections. In particular, in the case of KSHV, CRISPR-Cas9-mediated gene knockout enabled the identification of RSK, an important substrate of viral lytic protein ORF45 required for KSHV gene expression and production of virions (30, 31). Recently, a CRISPR-Cas9 screening was performed in 8 PEL cell lines (32). The results identified 210 essential genes across these cell lines and highlighted the dependence on IRF4 and MDM2 pathways in PEL survival. They also showed the dependency of PEL cells on cyclin D2 and c-Flip. In our study, we used matched primary MM cells as controls and identified 1,259 genes (group 8) that are essential for maintaining the proliferation of KMM cells, including 18 genes that had CRISPR score ratios of ≤5 (−32-fold) at day 21 over day 1 for KMM cells (Fig. 2). Among the top enriched pathways are those that are related to the mTOR pathway, which has been

FIG 5 Legend (Continued)
KMM cells after treatment with 1 μM KPT-8602 for 24 h analyzed by immunofluorescence assay. The sections were counterstained with DAPI, and pictures were taken with a confocal microscopy (magnification, ×600).

A

B   **C**
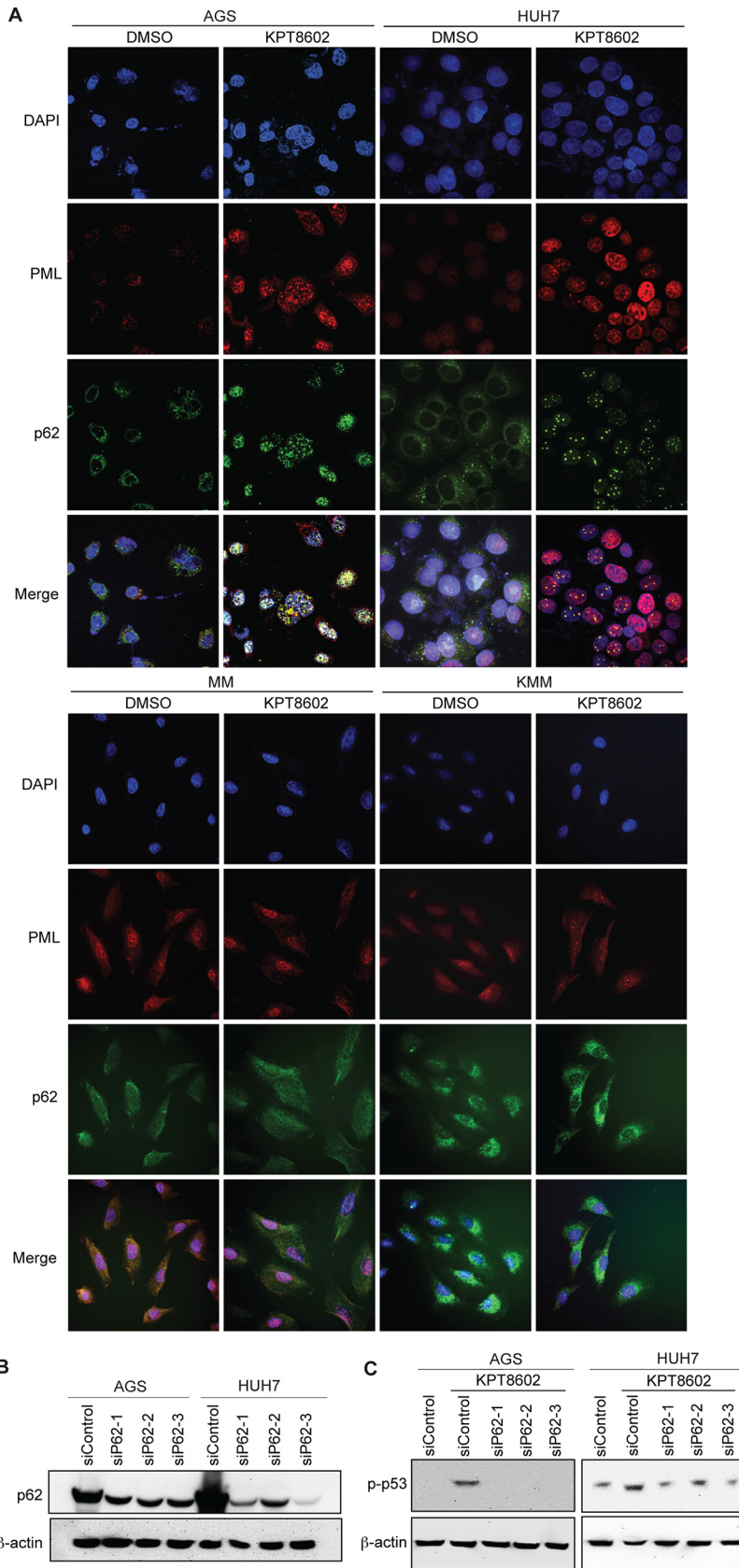
FIG 6 XPO1 inhibition-induced p53 activation in PML-NBs depends on p62 nuclear accumulation in AGS and HUH7 cells. (A) Expression of PML and p62 in AGS, HUH7, MM, and KMM cells after treatment with

(Continued on next page)

shown to be the most effective target in KS patients in clinical studies (18), thus validating the relevance of the model. These enriched pathways are likely vulnerable targets of KSHV-induced malignancies. In agreement with the PEL screening results, we identified IRF signaling as 1 of the 10 most highly enriched pathways, with genes losing sgRNAs in KMM cells over MM cells; however, the hypoxia signaling pathway and p38 MAPK pathway are the top enriched pathways with genes losing sgRNAs. These pathways have putative suppressive effects and hence are likely essential for maintaining the homeostasis of KSHV-transformed cells.

The current study identified XPO1 as a critical factor for the proliferation of KSHV-transformed cells. We confirmed the essential role of XPO1 in cell proliferation and cellular transformation of cell lines derived from gastric and liver cancers (Fig. 3). XPO1 dysregulation affects fundamental cellular processes such as inflammatory responses, cell cycle, and apoptosis and might contribute to tumorigenesis (2). Since numerous tumor suppressor proteins and oncoproteins, including p53, APC, Rb, NFAT, FOXO, p27, nucleophosmin, BCR-ABL, eIF4E, surviving, and β-catenin, harbor NES and are exported from the nucleus to the cytoplasm by XPO1 to fulfill their growth-promoting and antiapoptotic functions, nuclear-cytoplasmic transport, particularly transport mediated by XPO1, is likely an effective general target for cancer (2).

Upregulation of XPO1 is observed in many types of cancer tissues such as lung cancer, osteosarcoma, pancreatic cancer, ovarian cancer, cervical carcinoma, gastric and hepatocellular carcinoma, myeloid and lymphoid leukemia, mantle cell lymphoma, and multiple myeloma tissues (22). In parallel, XPO1 upregulation has been shown to affect the functions of several oncogenes such as vascular endothelial growth factor receptor (VEGF), epidermal growth factor (EGF) receptor, Cox-2, c-Myc, and HIF-1, which are not the direct cargos of XPO1 (33). In addition to XPO1 upregulation, posttranslational modifications of oncogenes and tumor suppressors can also alter or enhance their nuclear-cytoplasmic transport by XPO1. For example, p53 sumoylation and ubiquitination have been shown to enhance its XPO1-mediated export (34, 35). Drug resistance and poor prognosis have also been correlated with XPO1 upregulation in several malignancies (36, 37). For example, XPO1 upregulation induces aberrant nuclear-cytoplasmic export of topoisomerase IIα (Topo IIα) involved in DNA replication, transcription, and chromatin segregation. Topo IIα is a target of numerous anticancer drugs (38). However, its cytoplasmic export often induces resistance to Topo IIα-specific inhibitors such as doxorubicin and etoposide. As a result, XPO1 inhibition increases sensitivity to Topo IIα inhibitor (38). Hence, dual treatment with both Topo IIα inhibitor and XPO1 inhibitor is likely to improve the efficacy of cancer therapy.

The mechanism of XPO1 upregulation in cancer cells is still not well understood. Chromosomal translocations as well as mutations or gains of copies of the XPO1 gene could explain XPO1 overexpression. Indeed, a recurrent mutation in codon 571 of XPO1 gene has been reported in acute lymphoblastic leukemia (ALL) and in an adult with acute myeloid leukemia (AML) with CBL syndrome displaying XPO1 overexpression (39, 40). Moreover, Myc and p53, often found modulated in cancer cells, have been shown to positively and negatively alter the expression of XPO1, respectively (41). Finally, a copy number gain in the XPO1 locus was also observed in patients affected by primary mediastinal B-cell lymphoma (PMBL) and diffuse large B-cell lymphoma (DLBCL) (42, 43). We observed that there was an increase in XPO1 expression in KMM cells compared to MM cells and that both vCyclin and pre-miR-K3 mediated XPO1 upregulation (Fig. 3A to C). It would be interesting to investigate the effect of cell cycle progression on XPO1 upregulation.

FIG 6 Legend (Continued)
1 μM KPT-8602 for 24 h analyzed by immunofluorescence assay. The sections were counterstained with DAPI, and pictures were taken with a confocal microscopy (magnification, ×600). (B) Expression of p62 in AGS and HUH7 cells following siRNA knockdown analyzed by Western blotting. (C) Analysis of p-p53 in AGS and HUH7 cells after treatment with 1 μM KPT-8602 for 24 h following siRNA knockdown of p62 by Western blotting.

SINE compounds have been used to treat several types of cancer; among them, KPT-330 is currently in phase 1 and 2 clinical trials in numerous solid and hematologic malignancies with and without its use in combination with other chemotherapeutic agents and has shown promising results (33). To decrease adverse side effects, a second generation of SINE compounds that include KPT-8602 and that show improved tolerability has been developed and tested in clinical trials (44). In this report, we have shown that KPT-8602 inhibits the cell proliferation and cellular transformation of KMM, AGS, and HUH7 cells (Fig. 3), confirming the anticancer effect of members of the SINE family. Indeed, KPT-8602 has been shown to inhibit the proliferation of leukemia cells derived from ALL *in vitro* and to increase the animal survival rate in ALL xenograft models (45).

SINE compounds can block XPO1-mediated export and can therefore cause mislocalization of tumor suppressors or oncoproteins and decrease the rate of survival of cancer cells (1). A previous study highlighted the nuclear accumulation of p21, p27, and FOXO proteins after treatment with SINE compound S109 in colorectal cancer cells (46). Recently, KPT-330 has been shown to induce p53 and p21 retention within the nucleus in gastric cancer cells (47). In our study, we observed cell cycle arrest associated with p53 activation in KMM, AGS, and HUH7 cells after KPT-8602 treatment. However, we found that different types of cancer cells respond differently to this inhibitor, with KMM cells manifesting G_2/M arrest and AGS and HUH7 cells manifesting G_0/G_1 arrest (Fig. 4A). Consistent with these results, the mechanism mediating p53 activation in AGS and HUH7 cells is different from that in KMM cells. We have observed p53 nuclear accumulation in AGS and HUH7 cells but not in KMM cells after KPT-8602 treatment (Fig. 5B).

PML-NBs recruit a variety of proteins and modulate their posttranslational modifications. In particular, p53 and its regulators (ARF, HIPK2, CBP, MDM2, SIRT1, and MOZ) traffic through PML-NBs, suggesting that these nuclear bodies could regulate p53 activation by posttranslational modifications (48). Indeed, disruption of PML-NBs inhibits p53 activation and induces expression of its downstream genes, such as Bax and p21 (9, 49, 50); however, the underlying mechanism remains unclear. Interestingly, we have confirmed that p53 nuclear accumulation depends on the formation of PML-NBs after XPO1 inhibition in AGS and HUH7 cells (Fig. 4C to E). On the other hand, p53 activation in KMM after XPO1 inhibition does not depend on the formation of PML-NBs, which remains to be further explored.

Other NBs have been identified in the nucleus, and some studies suggested possible fusion events among them, forming hybrid NBs (51). Interestingly, XPO1 is involved in the formation of CRM1-nucleolar bodies (CNoBs), and its inhibition by XPO1 inhibitor leptomycin B disrupts CNoBs (52). Another type of NB involved with p62 (SQSTM1) was identified by imaging (26). p62 protein is mostly described as a scaffold cytoplasmic protein involved in autophagy processes by interacting with LC3, thereby mediating the recruitment of LC3 to polyubiquitinated protein aggregates to form autophagosome in the cytoplasm (53). Unlike its cytoplasmic function, the role of p62 within the nucleus is still not well understood. While PML-NBs are ubiquitous, CNoBs and p62-NBs are stress induced. It has been reported that p62-NBs are colocalized with PML-NBs upon inhibition of CNoBs (51), highlighting the role of nuclear p62 in the recruitment of polyubiquitinated proteins to PML-NBs (26).

The role of p62 in cancer development is still controversial (54). The expression level of p62 can be increased in cancer cells, and its overexpression has been shown to enhance cellular transformation through the activation of NRF2, mTORC1, and c-Myc pathways in liver cancer cells, independently of the autophagy pathway (55). On the other hand, in a nontumorigenic environment, p62 attenuates inflammation and fibrosis (56) and p62 loss has been shown to increase tumorigenesis in epithelial cells (57).

In this study, we demonstrated the essential role of p62 in the activation of the p53 tumor suppressor after XPO1 inhibition in AGS and HUH7 cells (Fig. 5 and 6). We observed nuclear accumulation of p62, which is colocalized with p53 after XPO1

inhibition in AGS and HUH7 cells. In parallel, we observed colocalization of p62 with PML-NBs, hence supporting the hypothesis of formation of PML-p62 hybrid NBs under stress conditions (26). Finally, we demonstrated for the first time that nuclear accumulation of p62 is required for p53 phosphorylation and activation within the PML-NBs after KPT-8602 treatment in AGS and HUH7 cells, demonstrating the indirect role of p62 in regulating the function of p53 in these cancer cells. Interestingly, while XPO1 inhibition causes an increase in the level of p62 in KMM cells, it neither leads to p62 nuclear accumulation nor mediates p53 activation (Fig. 5 and 6). It would be interesting to investigate whether the increase in the level of p62 after XPO1 inhibition contributes to the G_2/M cell cycle arrest in KMM cells.

MATERIALS AND METHODS

Cells and inhibitor. Rat primary embryonic mesenchymal stem cells (MM cells), KSHV-transformed MM cells (KMM cells), and AGS and HUH7 cell lines were maintained in Dulbecco modified Eagle medium (DMEM) supplemented with 10% fetal bovine serum (FBS; Sigma-Aldrich), 4 mM L-glutamine, and 10 μg/ml penicillin and streptomycin. KPT-8602 was obtained from Selleckchem.

Rat sgRNA library cloning. Rat sgRNA library cloning was carried out as previously described (58). This sgRNA library consists of a library of 59,520 unique sgRNAs targeting 19,840 coding genes, each with 3 independent sgRNAs, and 10 nontargeting sgRNAs, for a total of 59,530 sgRNAs. Specifically, we carefully chose three target sites for each gene to cover the most common exons in transcript variants ranging from 3% to 70% in the coding sequence (CDS) region from the rat genome (*Rattus norvegicus*; Rnor 5.0 version). Furthermore, we chose the target sites by avoiding potential off-target effects and in-frame mutations using Cas-OFFinder (59) and Cas-Designer (60) (http://www.rgenome.net/).

Lentiviral production of the sgRNA library. Lentiviral production was carried out as previously described (61, 62). Briefly, HEK293T cells were seeded at ~40% confluence 1 day before transfection in DMEM supplemented with 10% serum. One-hour prior to transfection, DMEM was removed and fresh Opti-MEM medium (Life Technologies) was added. Lipofectamine 2000 (Life Technologies) was used to transfect 20 μg of lentiCRISPR plasmid library, 10 μg of pVSVg, and 15 μg of psPAX2. Lipofectamine 2000 (100 μl) was diluted in 4 ml of Opti-MEM, and after 5 min, it was added to the mixture of plasmid DNAs, incubated for 20 min, and then added to the cells. The medium was refreshed after 6 h and collected after 3 days. The supernatant was centrifuged at 3,000 rpm at 4°C for 10 min to pellet cell debris, filtered (0.45-μm pore size), and concentrated by ultracentrifugation (Beckmann) at 24,000 rpm for 2 h at 4°C. The virus preparation was finally resuspended overnight at 4°C in DMEM, divided into aliquots, and stored at −80°C.

Lentiviral transduction of the sgRNA library. Lentiviral transduction was carried out as previously described (61). Cells were transduced with the short hairpin RNA (shRNA) library via "spinfection" at a multiplicity of infection (MOI) of 0.3 in full DMEM supplemented with 10% fetal bovine serum, 4 mM L-glutamine, and 10 μg/ml penicillin and streptomycin in the presence of 10 μg/ml of Polybrene. Flasks containing cells were centrifuged at 2,000 rpm for 2 h at 37°C. After the spin step, the medium was removed and fresh DMEM was added to the cells.

Genome DNA sequencing. Genome DNA sequencing was carried out as previously described (10). Genomic DNA was extracted using a QiAMP kit (Qiagen), and PCR was performed in two steps. First, the input genomic DNA was amplified in order to achieve 300× coverage over the sgRNA library using primers F1 (TCG TCG GCA GCG TCA GAT GTG TAT AAG AGA CAG TAT CTT GTG AAA GGA CGA AAA) and R1 (GTC TCG TGG GCT CGG AGA TGT GTA TAA GAG ACA GTT ATT TTA ACT TGC TAT TTC TAG CTC). Then, to attach Illumina adaptors and barcode samples, a second PCR was carried out using primers F2 (AAT GAT ACG GCG ACC ACC GAG ATC TAC ACT CTT TCC CTA CAC GAC GCT CTT CCG ATC T) and R2 (CAA GCA GAA GAC GGC ATA CGA GAT GTG ACT GGA GTT CAG ACG TGT GCT CTT CCG ATC T). Amplicons from the second PCR were subjected to gel extraction, quantified, mixed, and sequenced using a HiSeq 2500 instrument (Illumina).

Ingenuity pathway analysis. The pathways that were differentially enriched at day 21 over day 1 postransduction in KMM cells over MM cells were evaluated using IPA software (Ingenuity H Systems, USA).

Soft agar assay. Soft agar assay was carried out as previously described (15).

Cell proliferation assay. MM, KMM, AGS, and HUH7 cells plated at a density of 200,000 cells/well and treated with dimethyl sulfoxide (DMSO) or KPT-8602 at different concentrations were counted daily using a Malassez chamber.

Western blotting. Western blotting was carried out as previously described (62). Primary antibodies to β-actin (Santa Cruz), p62 (CST), SIRT1 (CST), Cas9-hemagglutinin (Cas9-HA; Santa Cruz), PML (CST), XPO1 (CST), p53 (CST), and phospho-p53 (CST) were used.

Immunofluorescence assay. Cells were fixed in methanol for 10 min at room temperature and processed for antibody staining as previously described (63). Immunostaining was performed using anti-p62 antibody (CST), anti-PML antibody (CST), or anti-phospho-p53 antibody (CST). Alexa488- and Alexa568-conjugated secondary antibodies (Thermo Fisher Scientific) were used to reveal the signals. Nuclei were counterstained with DAPI (4′,6-diamidino-2-phenylindole). Tissue sections that had not been subjected to incubation with primary antibodies were used as negative controls. Images of representative areas were acquired using a confocal fluorescence microscopy with a 60× objective (Nikon Eclipse C1).

Cell cycle assay. The cell cycle was analyzed as previously described (62). MM, KMM, AGS, and HUH7 cells pulsed with 10 μM 5-bromo-2′-deoxyuridine (BrdU) (B5002; Sigma-Aldrich) were stained with propidium iodide (P4864; Sigma-Aldrich). BrdU was detected by flow cytometry with a Pacific Blue-conjugated anti-BrdU antibody (B35129; Thermo Fisher Scientific). Results were analyzed using FlowJo software (FlowJo LLC, USA).

Statistical analysis. Statistical analysis was performed using the Kolmogorov-Smirnov test or the two-tailed t test as indicated in the figure legends, and a P value of $\leq$0.05 was considered significant. Single, double, and triple asterisks in the figures represent P values of $\leq$0.05, $\leq$0.01, and $\leq$0.001, respectively, while NS indicates that the results were not statistically significant.

Data availability. All CRISPR data generated in this study have been submitted to the NCBI Gene Expression Omnibus and will become publicly available with accession number GSE125507.

SUPPLEMENTAL MATERIAL

Supplemental material for this article may be found at https://doi.org/10.1128/mBio .00866-19.

FIG S1, TIF file, 0.5 MB.
FIG S2, TIF file, 0.7 MB.
FIG S3, TIF file, 0.3 MB.
TABLE S1, XLSX file, 1.4 MB.
TABLE S2, XLSX file, 0.02 MB.
TABLE S3, XLSX file, 0.03 MB.

ACKNOWLEDGMENTS

REFERENCES

1. Dickmanns A, Monecke T, Ficner R. 2015. Structural basis of targeting the exportin CRM1 in cancer. Cells 4:538–568. https://doi.org/10.3390/cells4030538.
2. Gravina GL, Senapedis W, McCauley D, Baloglu E, Shacham S, Festuccia C. 2014. Nucleo-cytoplasmic transport as a therapeutic target of cancer. J Hematol Oncol 7:85. https://doi.org/10.1186/s13045-014-0085-1.
3. Izaurralde E, Kutay U, von Kobbe C, Mattaj IW, Görlich D. 1997. The asymmetric distribution of the constituents of the Ran system is essential for transport into and out of the nucleus. EMBO J 16:6535–6547. https://doi.org/10.1093/emboj/16.21.6535.
4. Kabachinski G, Schwartz TU. 2015. The nuclear pore complex—structure and function at a glance. J Cell Sci 128:423–429. https://doi.org/10.1242/jcs.083246.
5. Okamura M, Inose H, Masuda S. 2015. RNA export through the NPC in eukaryotes. Genes (Basel) 6:124–149. https://doi.org/10.3390/genes6010124.
6. Fung HY, Chook YM. 2014. Atomic basis of CRM1—cargo recognition, release and inhibition. Semin Cancer Biol 27:52–61. https://doi.org/10.1016/j.semcancer.2014.03.002.
7. Gupta A, Saltarski JM, White MA, Scaglioni PP, Gerber DE. 2017. Therapeutic targeting of nuclear export inhibition in lung cancer. J Thorac Oncol 12:1446–1450. https://doi.org/10.1016/j.jtho.2017.06.013.
8. Chang HR, Munkhjargal A, Kim MJ, Park SY, Jung E, Ryu JH, Yang Y, Lim JS, Kim Y. 2018. The functional roles of PML nuclear bodies in genome maintenance. Mutat Res 809:99–107. https://doi.org/10.1016/j.mrfmmm.2017.05.002.
9. Guo A, Salomoni P, Luo J, Shih A, Zhong S, Gu W, Pandolfi PP. 2000. The function of PML in p53-dependent apoptosis. Nat Cell Biol 2:730–736. https://doi.org/10.1038/35036365.
10. Shalem O, Sanjana NE, Hartenian E, Shi X, Scott DA, Mikkelsen TS, Heckl D, Ebert BL, Root DE, Doench JG, Zhang F. 2014. Genome-scale CRISPR-Cas9 knockout screening in human cells. Science 343:84–87. https://doi.org/10.1126/science.1247005.
11. Zhou Y, Zhu S, Cai C, Yuan P, Li C, Huang Y, Wei W. 2014. High-throughput screening of a CRISPR/Cas9 library for functional genomics in human cells. Nature 509:487–491. https://doi.org/10.1038/nature13166.
12. Jinek M, Chylinski K, Fonfara I, Hauer M, Doudna JA, Charpentier E. 2012. A programmable dual-RNA-guided DNA endonuclease in adaptive bacterial immunity. Science 337:816–821. https://doi.org/10.1126/science.1225829.
13. Jones T, Ye F, Bedolla R, Huang Y, Meng J, Qian L, Pan H, Zhou F, Moody R, Wagner B, Arar M, Gao SJ. 2012. Direct and efficient cellular transformation of primary rat mesenchymal precursor cells by KSHV. J Clin Invest122:1076–1081. https://doi.org/10.1172/JCI58530.
14. Ye F, Lei X, Gao SJ. 2011. Mechanisms of Kaposi's sarcoma-associated herpesvirus latency and reactivation. Adv Virol 2011:1. https://doi.org/10.1155/2011/193860.
15. Jones T, Ramos da Silva S, Bedolla R, Ye F, Zhou F, Gao SJ. 2014. Viral cyclin promotes KSHV-induced cellular transformation and tumorigenesis by overriding contact inhibition. Cell Cycle 13:845–858. https://doi.org/10.4161/cc.27758.
16. Tan B, Liu H, Zhang S, da Silva SR, Zhang L, Meng J, Cui X, Yuan H, Sorel O, Zhang SW, Huang Y, Gao SJ. 2018. Viral and cellular N⁶-methyladenosine and N⁶,2′-O-dimethyladenosine epitranscriptomes in the KSHV life cycle. Nat Microbiol 3:108–120. https://doi.org/10.1038/s41564-017-0056-8.
17. Wang T, Birsoy K, Hughes NW, Krupczak KM, Post Y, Wei JJ, Lander ES, Sabatini DM. 2015. Identification and characterization of essential genes in the human genome. Science 350:1096–1101. https://doi.org/10.1126/science.aac7041.
18. Hosseini-Moghaddam SM, Soleimanirahbar A, Mazzulli T, Rotstein C, Husain S. 2012. Post renal transplantation Kaposi's sarcoma: a review of its epidemiology, pathogenesis, diagnosis, clinical aspects, and therapy. Transpl Infect Dis 14:338–345. https://doi.org/10.1111/j.1399-3062.2011.00714.x.
19. Chen C, Siegel D, Gutierrez M, Jacoby M, Hofmeister CC, Gabrail N, Baz R, Mau-Sorensen M, Berdeja JG, Savona M, Savoie L, Trudel S, Areethamsirikul N, Unger TJ, Rashal T, Hanke T, Kauffman M, Shacham S, Reece D. 2018. Safety and efficacy of selinexor in relapsed or refractory multiple

myeloma and Waldenstrom macroglobulinemia. Blood 131:855–863. https://doi.org/10.1182/blood-2017-08-797886.

20. Kuruvilla J, Savona M, Baz R, Mau-Sorensen PM, Gabrail N, Garzon R, Stone R, Wang M, Savoie L, Martin P, Flinn I, Jacoby M, Unger TJ, Saint-Martin JR, Rashal T, Friedlander S, Carlson R, Kauffman M, Shacham S, Gutierrez M. 2017. Selective inhibition of nuclear export with selinexor in patients with non-Hodgkin lymphoma. Blood 129:3175–3183. https://doi.org/10.1182/blood-2016-11-750174.

21. Garzon R, Savona M, Baz R, Andreeff M, Gabrail N, Gutierrez M, Savoie L, Mau-Sorensen PM, Wagner-Johnston N, Yee K, Unger TJ, Saint-Martin JR, Carlson R, Rashal T, Kashyap T, Klebanov B, Shacham S, Kauffman M, Stone R. 2017. A phase 1 clinical trial of single-agent selinexor in acute myeloid leukemia. Blood 129:3165–3174. https://doi.org/10.1182/blood-2016-11-750158.

22. Sun Q, Chen X, Zhou Q, Burstein E, Yang S, Jia D. 2016. Inhibiting cancer cell hallmark features through nuclear export inhibition. Signal Transduct Target Ther 1:16010. https://doi.org/10.1038/sigtrans.2016.10.

23. Moody R, Zhu Y, Huang Y, Cui X, Jones T, Bedolla R, Lei X, Bai Z, Gao SJ. 2013. KSHV microRNAs mediate cellular transformation and tumorigenesis by redundantly targeting cell growth and survival pathways. PLoS Pathog 9:e1003857. https://doi.org/10.1371/journal.ppat.1003857.

24. Li W, Jia X, Shen C, Zhang M, Xu J, Shang Y, Zhu K, Hu M, Yan Q, Qin D, Lee MS, Zhu J, Lu H, Krueger BJ, Renne R, Gao SJ, Lu C. 2016. A KSHV microRNA enhances viral latency and induces angiogenesis by targeting GRK2 to activate the CXCR2/AKT pathway. Oncotarget 7:32286–32305. https://doi.org/10.18632/oncotarget.8591.

25. Zheng Y, Gery S, Sun H, Shacham S, Kauffman M, Koeffler HP. 2014. KPT-330 inhibitor of XPO1-mediated nuclear export has anti-proliferative activity in hepatocellular carcinoma. Cancer Chemother Pharmacol 74:487–495. https://doi.org/10.1007/s00280-014-2495-8.

26. Pankiv S, Lamark T, Bruun JA, Overvatn A, Bjorkoy G, Johansen T. 2010. Nucleocytoplasmic shuttling of p62/SQSTM1 and its role in recruitment of nuclear polyubiquitinated proteins to promyelocytic leukemia bodies. J Biol Chem 285:5941–5953. https://doi.org/10.1074/jbc.M109.039925.

27. Mosbach V, Poggi L, Richard GF. 2019. Trinucleotide repeat instability during double-strand break repair: from mechanisms to gene therapy. Curr Genet 65:17–28. https://doi.org/10.1007/s00294-018-0865-1.

28. Ganem D. 2010. KSHV and the pathogenesis of Kaposi sarcoma: listening to human biology and medicine. J Clin Invest 120:939–949. https://doi.org/10.1172/JCI40567.

29. Gilani U, Shaukat M, Rasheed A, Shahid M, Tasneem F, Arshad M, Rashid N, Shahzad N. 2019. The implication of CRISPR/Cas9 genome editing technology in combating human oncoviruses. J Med Virol 91:1–13. https://doi.org/10.1002/jmv.25292.

30. van Diemen FR, Lebbink RJ. 2017. CRISPR/Cas9, a powerful tool to target human herpesviruses. Cell Microbiol 19(2). https://doi.org/10.1111/cmi.12694.

31. Avey D, Tepper S, Li W, Turpin Z, Zhu F. 2015. Phosphoproteomic analysis of KSHV-infected cells reveals roles of ORF45-activated RSK during lytic replication. PLoS Pathog 11:e1004993. https://doi.org/10.1371/journal.ppat.1004993.

32. Manzano M, Patil A, Waldrop A, Dave SS, Behdad A, Gottwein E. 2018. Gene essentiality landscape and druggable oncogenic dependencies in herpesviral primary effusion lymphoma. Nat Commun 9:3263. https://doi.org/10.1038/s41467-018-05506-9.

33. Ishizawa J, Kojima K, Hail N, Jr, Tabe Y, Andreeff M. 2015. Expression, function, and targeting of the nuclear exporter chromosome region maintenance 1 (CRM1) protein. Pharmacol Ther 153:25–35. https://doi.org/10.1016/j.pharmthera.2015.06.001.

34. Lohrum MA, Woods DB, Ludwig RL, Balint E, Vousden KH. 2001. C-terminal ubiquitination of p53 contributes to nuclear export. Mol Cell Biol 21:8521–8532. https://doi.org/10.1128/MCB.21.24.8521-8532.2001.

35. Santiago A, Li D, Zhao LY, Godsey A, Liao D. 2013. p53 SUMOylation promotes its nuclear export by facilitating its release from the nuclear export receptor CRM1. Mol Biol Cell 24:2739–2752. https://doi.org/10.1091/mbc.E12-10-0771.

36. Huang WY, Yue L, Qiu WS, Wang LW, Zhou XH, Sun YJ. 2009. Prognostic value of CRM1 in pancreas cancer. Clin Invest Med 32:E315.

37. Noske A, Weichert W, Niesporek S, Roske A, Buckendahl AC, Koch I, Sehouli J, Dietel M, Denkert C. 2008. Expression of the nuclear export protein chromosomal region maintenance/exportin 1/Xpo1 is a prognostic factor in human ovarian cancer. Cancer 112:1733–1743. https://doi.org/10.1002/cncr.23354.

38. Nitiss JL. 2009. Targeting DNA topoisomerase II in cancer chemotherapy. Nat Rev Cancer 9:338–350. https://doi.org/10.1038/nrc2607.

39. Puente XS, Pinyol M, Quesada V, Conde L, Ordóñez GR, Villamor N, Escaramis G, Jares P, Beà S, González-Díaz M, Bassaganyas L, Baumann T, Juan M, López-Guerra M, Colomer D, Tubío JMC, López C, Navarro A, Tornador C, Aymerich M, Rozman M, Hernández JM, Puente DA, Freije JMP, Velasco G, Gutiérrez-Fernández A, Costa D, Carrió A, Guijarro S, Enjuanes A, Hernández L, Yagüe J, Nicolás P, Romeo-Casabona CM, Himmelbauer H, Castillo E, Dohm JC, de Sanjosé S, Piris MA, de Alava E, San Miguel J, Royo R, Gelpí JL, Torrents D, Orozco M, Pisano DG, Valencia A, Guigó R, Bayés M, et al. 2011. Whole-genome sequencing identifies recurrent mutations in chronic lymphocytic leukaemia. Nature 475:101–105. https://doi.org/10.1038/nature10113.

40. Luthra R, Patel KP, Reddy NG, Haghshenas V, Routbort MJ, Harmon MA, Barkoh BA, Kanagal-Shamanna R, Ravandi F, Cortes JE, Kantarjian HM, Medeiros LJ, Singh RR. 2014. Next-generation sequencing-based multi-gene mutational screening for acute myeloid leukemia using MiSeq: applicability for diagnostics and disease monitoring. Haematologica 99:465–473. https://doi.org/10.3324/haematol.2013.093765.

41. Golomb L, Bublik DR, Wilder S, Nevo R, Kiss V, Grabusic K, Volarevic S, Oren M. 2012. Importin 7 and exportin 1 link c-Myc and p53 to regulation of ribosomal biogenesis. Mol Cell 45:222–232. https://doi.org/10.1016/j.molcel.2011.11.022.

42. Lenz G, Wright GW, Emre NC, Kohlhammer H, Dave SS, Davis RE, Carty S, Lam LT, Shaffer AL, Xiao W, Powell J, Rosenwald A, Ott G, Muller-Hermelink HK, Gascoyne RD, Connors JM, Campo E, Jaffe ES, Delabie J, Smeland EB, Rimsza LM, Fisher RI, Weisenburger DD, Chan WC, Staudt LM. 2008. Molecular subtypes of diffuse large B-cell lymphoma arise by distinct genetic pathways. Proc Natl Acad Sci U S A 105:13520–13525. https://doi.org/10.1073/pnas.0804295105.

43. Jardin F, Pujals A, Pelletier L, Bohers E, Camus V, Mareschal S, Dubois S, Sola B, Ochmann M, Lemonnier F, Viailly PJ, Bertrand P, Maingonnat C, Traverse-Glehen A, Gaulard P, Damotte D, Delarue R, Haioun C, Argueta C, Landesman Y, Salles G, Jais JP, Figeac M, Copie-Bergman C, Molina TJ, Picquenot JM, Cornic M, Fest T, Milpied N, Lemasle E, Stamatoullas A, Moeller P, Dyer MJ, Sundstrom C, Bastard C, Tilly H, Leroy K. 2016. Recurrent mutations of the exportin 1 gene (XPO1) and their impact on selective inhibitor of nuclear export compounds sensitivity in primary mediastinal B-cell lymphoma. Am J Hematol 91:923–930. https://doi.org/10.1002/ajh.24451.

44. Hing ZA, Fung HY, Ranganathan P, Mitchell S, El-Gamal D, Woyach JA, Williams K, Goettl VM, Smith J, Yu X, Meng X, Sun Q, Cagatay T, Lehman AM, Lucas DM, Baloglu E, Shacham S, Kauffman MG, Byrd JC, Chook YM, Garzon R, Lapalombella R. 2016. Next-generation XPO1 inhibitor shows improved efficacy and in vivo tolerability in hematological malignancies. Leukemia 30:2364–2372. https://doi.org/10.1038/leu.2016.136.

45. Vercruysse T, De Bie J, Neggers JE, Jacquemyn M, Vanstreels E, Schmid-Burgk JL, Hornung V, Baloglu E, Landesman Y, Senapedis W, Shacham S, Dagklis A, Cools J, Daelemans D. 2017. The second-generation exportin-1 inhibitor KPT-8602 demonstrates potent activity against acute lymphoblastic leukemia. Clin Cancer Res 23:2528–2541. https://doi.org/10.1158/1078-0432.CCR-16-1580.

46. Niu M, Chong Y, Han Y, Liu X. 2015. Novel reversible selective inhibitor of nuclear export shows that CRM1 is a target in colorectal cancer cells. Cancer Biol Ther 16:1110–1118. https://doi.org/10.1080/15384047.2015.1047569.

47. Subhash VV, Yeo MS, Wang L, Tan SH, Wong FY, Thuya WL, Tan WL, Peethala PC, Soe MY, Tan DSP, Padmanabhan N, Baloglu E, Shacham S, Tan P, Koeffler HP, Yong WP. 2018. Anti-tumor efficacy of Selinexor (KPT-330) in gastric cancer is dependent on nuclear accumulation of p53 tumor suppressor. Sci Rep 8:12248. https://doi.org/10.1038/s41598-018-30686-1.

48. Garcia PB, Attardi LD. 2014. Illuminating p53 function in cancer with genetically engineered mouse models. Semin Cell Dev Biol 27:74–85. https://doi.org/10.1016/j.semcdb.2013.12.014.

49. Pearson M, Carbone R, Sebastiani C, Cioce M, Fagioli M, Saito S, Higashimoto Y, Appella E, Minucci S, Pandolfi PP, Pelicci PG. 2000. PML regulates p53 acetylation and premature senescence induced by oncogenic Ras. Nature 406:207–210. https://doi.org/10.1038/35018127.

50. Fogal V, Gostissa M, Sandy P, Zacchi P, Sternsdorf T, Jensen K, Pandolfi PP, Will H, Schneider C, Del Sal G. 2000. Regulation of p53 activity in nuclear bodies by a specific PML isoform. EMBO J 19:6185–6195. https://doi.org/10.1093/emboj/19.22.6185.

51. Souquere S, Weil D, Pierron G. 2015. Comparative ultrastructure of

CRM1-nucleolar bodies (CNoBs), intranucleolar bodies (INBs) and hybrid PML/p62 bodies uncovers new facets of nuclear body dynamic and diversity. Nucleus 6:326–338. https://doi.org/10.1080/19491034.2015.1082695.

52. Ernoult-Lange M, Wilczynska A, Harper M, Aigueperse C, Dautry F, Kress M, Weil D. 2009. Nucleocytoplasmic traffic of CPEB1 and accumulation in Crm1 nucleolar bodies. Mol Biol Cell 20:176–187. https://doi.org/10.1091/mbc.e08-09-0904.

53. Pankiv S, Clausen TH, Lamark T, Brech A, Bruun JA, Outzen H, Overvatn A, Bjorkoy G, Johansen T. 2007. p62/SQSTM1 binds directly to Atg8/LC3 to facilitate degradation of ubiquitinated protein aggregates by autophagy. J Biol Chem 282:24131–24145. https://doi.org/10.1074/jbc.M702824200.

54. Moscat J, Karin M, Diaz-Meco MT. 2016. p62 in cancer: signaling adaptor beyond autophagy. Cell 167:606–609. https://doi.org/10.1016/j.cell.2016.09.030.

55. Umemura A, He F, Taniguchi K, Nakagawa H, Yamachika S, Font-Burgada J, Zhong Z, Subramaniam S, Raghunandan S, Duran A, Linares JF, Reina-Campos M, Umemura S, Valasek MA, Seki E, Yamaguchi K, Koike K, Itoh Y, Diaz-Meco MT, Moscat J, Karin M. 2016. p62, upregulated during preneoplasia, induces hepatocellular carcinogenesis by maintaining survival of stressed HCC-initiating cells. Cancer Cell 29:935–948. https://doi.org/10.1016/j.ccell.2016.04.006.

56. Zhong Z, Umemura A, Sanchez-Lopez E, Liang S, Shalapour S, Wong J, He F, Boassa D, Perkins G, Ali SR, McGeough MD, Ellisman MH, Seki E, Gustafsson AB, Hoffman HM, Diaz-Meco MT, Moscat J, Karin M. 2016. NF-kappaB restricts inflammasome activation via elimination of damaged mitochondria. Cell 164:896–910. https://doi.org/10.1016/j.cell.2015.12.057.

57. Valencia T, Kim JY, Abu-Baker S, Moscat-Pardos J, Ahn CS, Reina-Campos M, Duran A, Castilla EA, Metallo CM, Diaz-Meco MT, Moscat J. 2014. Metabolic reprogramming of stromal fibroblasts through p62-mTORC1 signaling promotes inflammation and tumorigenesis. Cancer Cell 26:121–135. https://doi.org/10.1016/j.ccr.2014.05.004.

58. Kim HS, Lee K, Bae S, Park J, Lee CK, Kim M, Kim E, Kim M, Kim S, Kim C, Kim JS. 2017. CRISPR/Cas9-mediated gene knockout screens and target identification via whole-genome sequencing uncover host genes required for picornavirus infection. J Biol Chem 292:10664–10671. https://doi.org/10.1074/jbc.M117.782425.

59. Bae S, Park J, Kim JS. 2014. Cas-OFFinder: a fast and versatile algorithm that searches for potential off-target sites of Cas9 RNA-guided endonucleases. Bioinformatics 30:1473–1475. https://doi.org/10.1093/bioinformatics/btu048.

60. Park J, Bae S, Kim JS. 2015. Cas-Designer: a web-based tool for choice of CRISPR-Cas9 target sites. Bioinformatics 31:4014–4016. https://doi.org/10.1093/bioinformatics/btv537.

61. Cho SW, Kim S, Kim JM, Kim JS. 2013. Targeted genome engineering in human cells with the Cas9 RNA-guided endonuclease. Nat Biotechnol 31:230–232. https://doi.org/10.1038/nbt.2507.

62. He M, Tan B, Vasan K, Yuan H, Cheng F, Ramos da Silva S, Lu C, Gao SJ. 2017. SIRT1 and AMPK pathways are essential for the proliferation and survival of primary effusion lymphoma cells. J Pathol 242:309–321. https://doi.org/10.1002/path.4905.

63. Yuan H, Tan B, Gao SJ. 2017. Tenovin-6 impairs autophagy by inhibiting autophagic flux. Cell Death Dis 8:e2608. https://doi.org/10.1038/cddis.2017.25.